Extended Abstracts of

The First International Workshop on Junction Technology

December 6, 2000
Makuhari, Chiba, Japan
Makuhari Prince Hotel

Sponsored by
The Japan Society of Applied Physics
Silicon Technology Division

Tecnical Cosponsored by
IEEE Electron Devices Society

Sponsored by
SEMI Japan
Highly Functionalized Global Interface Integration Research Project
IEEE EDS Japan Chapter
ECS Japan Local Section
PDUG: Plasma Doping Users Group

Cosponsored by
IEICE Silicon Devices and Materials
Japan Society for the Promotion of Science, The 131and 165 Committee
STRJ: Semiconductor Technology Roadmap Committee of Japan
STARC: Semiconductor Technology Academic Research Center
Selete: Semiconductor Leading Edge Technologies, Inc.

In Cooperation with
IEEJ Technical Meeting on Electron Devices
NEDO: New Energy and Industrial Technology Development Organization

Plasma Doping: Theoretical Simulation and Use of Safer Gas

Paul K. Chu

Department of Physics & Materials Science
City University of Hong Kong
83 Tat Chee Avenue, Kowloon, Hong Kong
(E-mail: paul.chu@cityu.edu.hk)

Abstract

Plasma doping (PD) is an alternative technique to form shallow junctions in deep sub-micrometer microelectronic devices. The use of theoretical simulation to derive the energy distribution of implanted ions can lessen the time required for designing PD experiments and recipes. It also provides useful information on the dopant depth profiles. The second part of the paper describes the use of a boron-containing gas that is much less toxic than diborane to form shallow junctions.

Theoretical Simulation

Plasma doping (PD) has been demonstrated to produce junctions as shallow as those by low energy beam-line ion implantation or beam-line doping (BD). PD is more efficient and economical than BD as the entire wafer can be implanted simultaneously in PD and PD equipment is simpler [1,2]. It has been shown that microelectronic devices fabricated by PD have higher drive current [3]. In addition, cross-sectional transmission electron microscopy (XTEM) shows that even though high dose BF_3 PD or BD renders the silicon surface amorphous and indistinguishable by XTEM, there is less residual damage after rapid thermal annealing in PD devices [4]. It is one of the interesting and beneficial factors favoring PD in ultra shallow junction formation.

PD differs significantly from conventional beam-line implantation in several aspects [5,6]. In beam-line implantation, the ions are accelerated and filtered according to their mass-to-charge ratio. Therefore, with sufficient mass resolution, the output "beam-line" ions are unique in mass, charge state, and impact energy. In PD, the target is immersed in a plasma, and a series of negative voltage pulses are applied to the target to conduct implantation. When the target is negatively biased, electrons are repelled away from the sample surface almost instantaneously creating a sheath of heavy positive ions. An electric field is established between the sheath boundary and target surface, and positive ions are accelerated towards the target with the applied voltage provided that the gas pressure is low enough so that collisionless conditions are satisfied (that is, ion mean free path >> sheath thickness). To maintain the continuous flow of ions, the ion sheath expands until the end of the negative pulse or an equilibrium is reached. It should also be noted that the ion impact angle and implant dose uniformity depend on the shape of the target and to some extent the sample holder [7,8].

There are several ways to alter the impact energy of the ions in PD. The plasma is usually composed of ion species with different masses and charge states. The higher the charge state, the bigger is the impact energy. In most plasma conditions, there is one dominant ion species, for example, BF_2^+ in a BF_3 plasma. There is also a short period of rise and fall time at the beginning and end of each negative voltage pulse. During these periods, ions do not receive the full acceleration. As a result, the ion impact energy distribution and depth profile of a PD sample is intrinsically different from that of a conventional BD sample.

In this work, a one-dimensional particle-in-cell (PIC) model [9-11] is used to simulate BF_3 PD into a silicon wafer under different pulsing conditions. We compare the depth profiles of PD (BF_3 plasma consisting of 70% BF_2^+, 10% BF_3^+, 10% BF^+, and 10% of B^+) with those of BD simulated by the TRIM code (100% BF_2^+) [12]. It

ISBN 4-89114-008-9/009-7

is observed that the implant peak is shallower in PD at the same implantation energy even for the zero rise and fall time case primarily due to the presence of multiple species in a BF_3 plasma. For finite rise and full time, there exists a large surface peak not present in BD samples. These low energy ions favor the formation of good ohmic contacts and are the biggest discernable difference between PD and BD. In spite of their low energy, these ions can also cause subtle differences in the nature of the surface layer and are speculated to be the primary reason for the reduced residual damage after rapid thermal annealing reported by Takase, et al. [4]

In our simulation, the waveform of each voltage pulse is divided into three intervals: rise time, steady-state or constant voltage period, and fall time. For simplicity, the steady-state period is set as 10 μsec. Rise and fall times of 0, 1, 3, and 5 μsec are used in the simulation giving the final pulse duration of 10, 12, 16, and 20 μsec. Based on mass spectrometric measurement of the BF_3 plasma in our instrument, we set the plasma composition to be 70% BF_2^+, 10% BF_3^+, 10% BF^+, and 10% of B^+ in our model. The plasma density is 5.0×10^9 cm^{-3}, i.e., 3.5×10^9 cm^{-3} BF_2^+, 5.0×10^8 cm^{-3} BF_3^+, 5.0×10^8 cm^{-3} BF^+, and 5.0×10^8 cm^{-3} B^+. The "collisionless" conditions are fulfilled due to the low working gas pressure. To accentuate the effects of the rise and fall time, we choose a sample voltage of –5kV. The potential, ϕ, is related to the four ion densities, n_{BF_3}, n_{BF_2}, n_{BF}, n_B, and electron density, n_e, by Poisson's equation:

$$\nabla^2\phi = -\frac{\left(n_{BF_3} + n_{BF_2} + n_{BF} + n_B - n_e\right)}{\varepsilon_o} \qquad \text{(Eq. 1)}$$

where ε_o is the dielectric constant. The electron temperature T_e is 2eV, and n_e is given by Boltzmann's function:

$$n_e = n_o \exp\left(\frac{q\phi}{T_e}\right) \qquad \text{(Eq. 2)}$$

where q is the elemental charge. The potential, ϕ, is solved by Eq. 1 and finite difference. The acceleration, a, initial velocity, v_i, final velocity, v_f, and displacement, x, of each ion species within a time step, Δt, are derived by Newton's equations:

$$v_f = v_i + a\Delta t \qquad \text{(Eq. 3a)}$$

$$x = v_i\Delta t + \frac{1}{2}a(\Delta t)^2 \qquad \text{(Eq. 3b)}$$

A total of 240,000 particles, 60,000 for each species, are used in the simulation. Each particle represents 583333 cm^{-2} density for BF_2^+, 83333 cm^{-2} density for BF_3^+, 83333 cm^{-2} density for BF^+, 83333 cm^{-2} density for B^+. The grid spacing is 5×10^{-2} cm and the time step is 1.4×10^{-4} μs.

Fig. 1 displays the histogram of the simulated energy distribution of the implanted ions. The relative concentration of low energy ions (below 2.5keV) is 7.4% for a zero rise and fall time pulse. These ions are initially quite close to the surface of the silicon wafer and do not receive the full acceleration during the rapid sheath expansion. The contribution of low energy ions is higher for a longer pulse width and they are implanted mainly during the rise and fall time of the negative pulse. The relative proportion of this low energy component rises to 18.7% for 1μs, 26.5% for 3μs, and 30.5% for 5μs rise and fall time pulses. For a longer rise and fall time, the ratio of the combined duration of the rise and fall time to that of the total pulse is larger, and the proportion of these low energy ions is thus bigger.

The simulated boron depth profiles for pulse widths of 10μs, 12μs, 16μs, and 20μs are depicted in Fig. 2. Each depth profile is calculated by summing the weighted contributions at different energies and ions according to Fig. 1. The net impact energy of B is 11/49 of the sample bias for BF_2^+ ions. We use a Gaussian distribution (Eq. 4):

$$N(x) = \sum N_i(x) = \sum \frac{d_i}{\sqrt{2\pi}\Delta R_p} \exp\left[\frac{-(x-R_p)^2}{2\Delta R_p^2}\right]$$

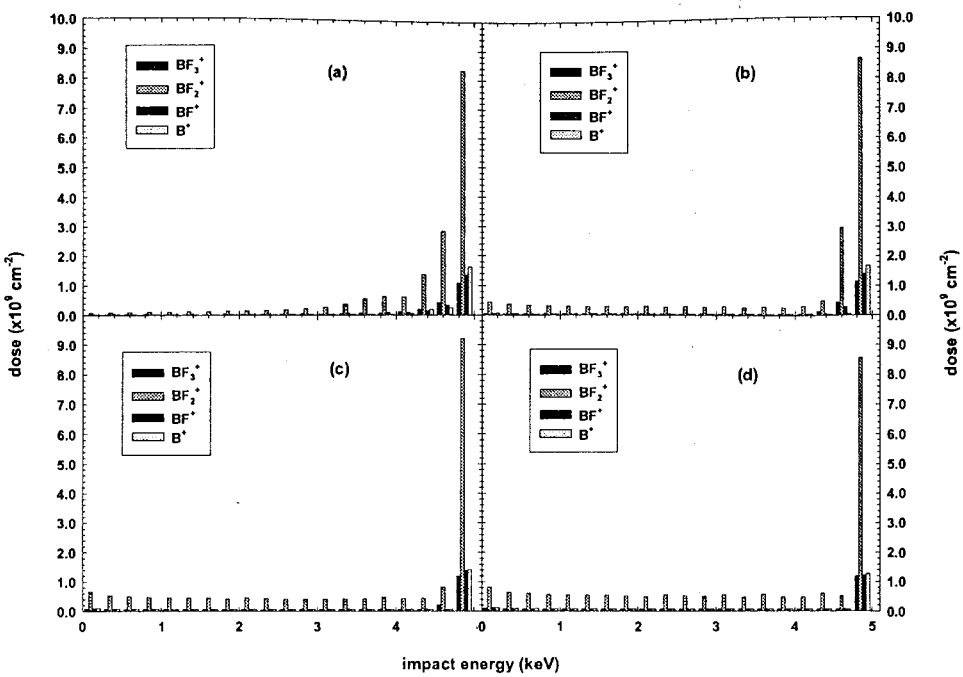

Fig. 1 Histograms of the simulated energy distribution of the implanted ions using (a) zero, (b) 1 μs, (c) 3 μs, and (d) 5 μs rise and fall time. The steady-state (constant voltage) period of the pulse is 10 μs.

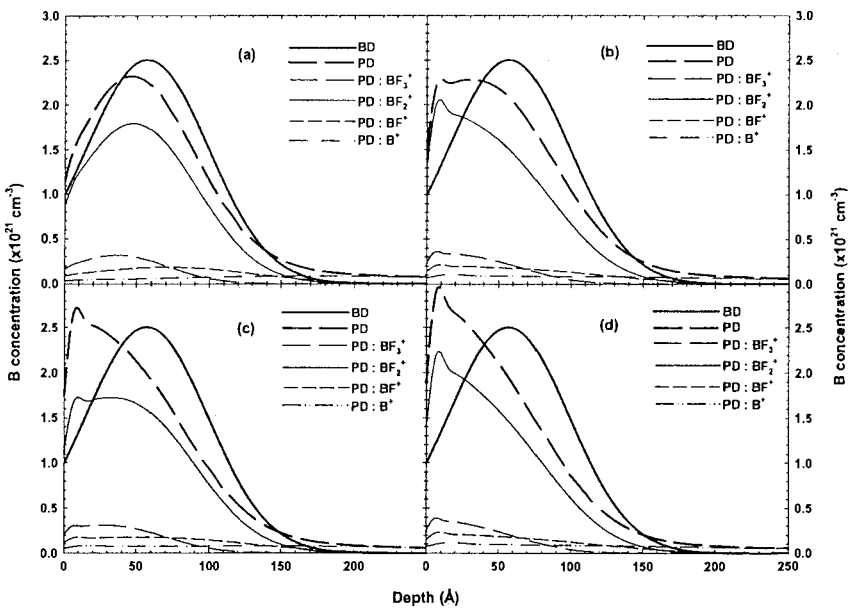

Fig. 2 Simulated depth profiles of implanted boron for different pulse durations: (a) zero, (b) 1 μs, (c) 3 μs, and (d) 5 μs rise and fall time. The steady-state (constant voltage) period of the pulse is 10 μs. The B profile in beam-line BF_2^+ implant is shown for comparison.

ISBN 4-89114-008-9/009-7

where $N_i(x)$, d_i , R_p, and ΔR_p are the concentration, dose, projected range, and standard deviation, respectively for each implant energy and ion. The TRIM code is employed to obtain the projected range, R_p, and standard deviation, ΔR_p, at each implant energy.

The B depth profiles generated for the zero rise and fall time PD case are displayed in Fig. 2a. Comparing to BD, the PD profiles are shallower and more skewed towards the surface. In reality, no power modulator is perfect and the rise and fall time of the voltage pulse is always nonzero. As the rise and fall time increases, the depth profile dramatically changes from a near-Gaussian distribution to a broad distribution skewed towards the surface and a sharp surface peak also results as shown in Figs. 2b to 2d. The surface peak becomes sharper and more prominent at longer rise and fall time since this extremely low energy ion component (below 1keV) increases from 2.4% at zero rise and fall time to 8.5% at 1μs, 12.0% at 3μs, and 13.8% at 5μs.

As shown in our simulation results, an almost flat-top dopant profile with a surface spike can be achieved by tailoring the voltage pulse shape, and one can obtain doping profiles that are extremely difficult via BD. The existence of such a surface peak which has been shown experimentally [1,4,13] may be advantageous to the formation of low resistance contacts for ultra shallow junctions.

Based on our results, the biggest discernable difference between PD and BD is the low energy component. It is speculated to be the primary reason why PD samples show less residual defects after rapid thermal annealing. Even though XTEM discloses that the surface layers in both high dose BF_3 BD and PD samples have been amorphized [4], the concentration of these low energy ions is quite large in PD with finite rise and fall time. Their presence in the surface layer and the extra surface damage created facilitate more effective regrowth during subsequent rapid thermal annealing. A longer rise and fall time increases this surface component and may be preferred in the formation of shallow junctions. As a short voltage pulse alleviates sample charging on patterned wafers [13], we propose that for plasma doping, the optimal voltage pulse should have a short duration with relatively long rise and fall time. This is not something easily attainable by conventional beam-line ion implantation.

Use of Safer Gas

Because of the absence of ion transportation optics and mass selection, plasma doping yields a high ion flux at a low cost. However, due to the lack of mass separation mechanism, all ions in the chamber will be co-implanted. In plasma doping, the doping gases are normally diluted with nitrogen, hydrogen, or helium for safety precaution as the common doping gases such as diborane are extremely toxic. Being highly flammable, diborane may explode from heat, shock, or friction. It can cause respiratory tract burns as well as skin and eye irritation. Diborane is fatal if inhaled. It is corrosive and hydrolyzed in the lungs causing pulmonary edema and possible hemorrhaging. Although such hydride gases are commonly employed in conventional ion implanters, the actual volume is small because it is only used in the arc chamber of the ion source. On the other hand, the volume used in plasma doping chambers is much larger especially for 300mm wafers. While every plasma doping system employs extreme safety measures, one must take into consideration the ramifications that may result in case of exposure due to a gas leak or accident. Using the least dangerous gas would be the obvious choice. Even though the less toxic BF_3 gas has been used in plasma doping experiments, the high etching rate of F can be a drawback in some applications [14]. Therefore, there is a definite need to search for a safer and better doping gas in plasma doping experiments.

Borazine ($B_3N_3H_6$) that is commercially available only recently (from Boron Biologicals) is

a hopeful candidate. In the worst case, borazine vapors may cause irritation to the skin, eyes, and mucous membranes. It is not listed in the National Toxicology Program (NTP) and found not to be a potential carcinogen in the International Agency for Research on Cancer (IARC). Although borazine does pose some minor dangers, they pale in comparison to diborane. Since borazine is a new doping gas, the first logical step is to investigate the feasibility by observing the doping profiles.

Our experiments were conducted in a plasma doping instrument equipped with a microwave source powered by an ENI OEM-12A 1400W solid state power generator and a matching network [15]. The power was transmitted via the tuner into the chamber through a quartz window. A stainless steel wafer holder was located 4 cm above the bottom in the center line of the chamber and biased by a negative high voltage pulse generator. After a 6-inch silicon wafer was placed on the wafer holder, the chamber was pumped down to a base pressure in the low 10^{-6} Torr range. A working pressure of 3 millitorr was obtained by injecting a gas mixture of N_2 and 5% borazine into the chamber. Nitrogen was used in our experiments as a diluting gas that also helps to amorphize the silicon substrate to prevent channeling. A series of pulsed negative bias with different voltages was then applied into the wafer holder in order to achieve the more desirable shallow, flat-top boron distribution. The pulsing rate was 1000 pulses per second and the gate width was 3 microseconds. The experimental parameters are presented in Table 1.

Fig. 1 depicts the secondary ion mass spectrometry (SIMS) depth profile of boron and silicon (matrix marker) of our first experiment using 5% borazine. Instead of a doping profile showing an exponential decay, the data show that the boron concentration is very high and more or less constant extending to a depth of about 0.3 μm. In this surface region, the silicon concentration is quite low. It thus appears that boron has been deposited instead of implanted, and electrical tests on this sample show poor surface conductivity. After some experimental investigations, we found that the solution was to lower the borazine concentration and shorten the process time. Therefore, in subsequent experiments, the pressure was maintained at 3 millitorr but the borazine concentration was reduced to 1 percent diluted by nitrogen. To achieve the same boron dose with shorter exposure time, we adjusted the pulse rate to $10x10^3$ pulses per second. Fig. 2 depicts the SIMS result of the sample implanted using the latter conditions revealing the expected doping profile.

TABLE 1
EXPERIMENTAL CONDITIONS

Applied Voltage (volt)	Boron Dose (x 10^{14} cm^{-3})	Effective Implantation Time (seconds)
500	1.1	6.83
700	1.0	6.55
800	2.9	15.99
900	4.3	20.83
1000	0.69	3.46

Our results demonstrate that borazine plasma doping can yield boron in-depth distributions similar to those using other more toxic doping gases such as diborane and boron trifluoride. However, unlike other doping gases, our experiments show that if the borazine pressure is too high, boron deposition instead of implantation can occur. The optimal concentration window is about 1%, and more investigation must be conducted to understand the competition between boron deposition and implantation in borazine plasma doping.

Acknowledgments

The author acknowledges the contribution from D. T. K. Kwok, L. M. Fang, and J. Genevich. The work was jointly supported by Hong Kong RGC

ISBN 4-89114-008-9/009-7

CERG 9040344, 9040412, 9040498 and City University of Hong Kong SRG 7001028.

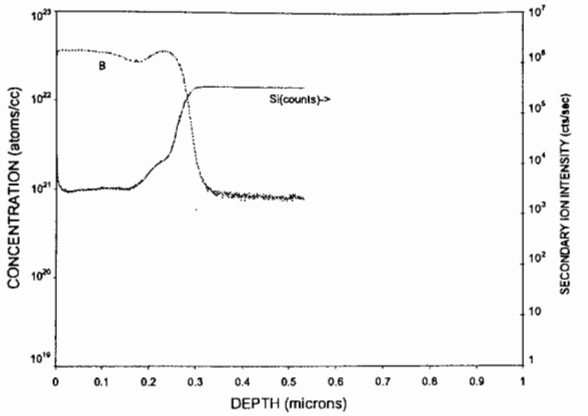

Fig. 3 Secondary ion mass spectrometry (SIMS) depth profiles acquired from the sample implanted using 5% borazine. Silicon is plotted as secondary ion intensities.

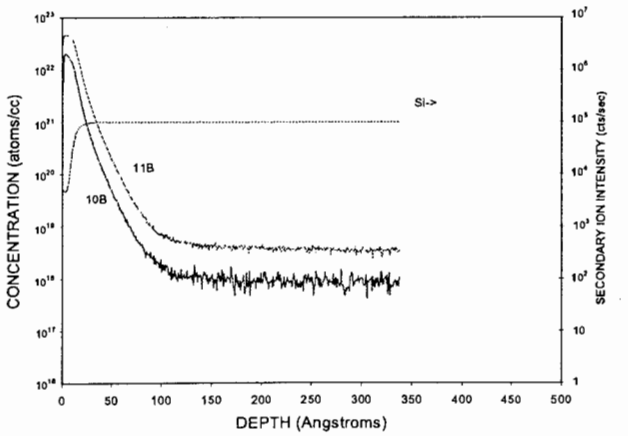

Fig. 4 Secondary ion mass spectrometry (SIMS) depth profiles acquired from the samples implanted using 1% borazine. Silicon is plotted as secondary ion intensities.

References

[1] P. K. Chu, S. B. Felch, P. Kellerman, F. Sinclair, L. A. Larson, and B. Mizuno, Solid State Technol., **42(9)**, 55 (1999); **42(10)**, 77 (1999).

[2] M. J. Goeckner, S. B. Felch, J. Weeman, S. Mehta, and J. S. Reedholm, J. Vac. Sci. Technol. A, 17, 1501 (1999).

[3] M. J. Goeckner, S. B. Felch, Z. Fang, D. Lenoble, J. Galvier, A. Grouillet, G. C.-R. Yeap, D. Bang, and M.-R. Lin, J. Vac. Sci. Technol. B, **17(5)**, 2290 (1999).

[4] M. Takase, K. Yamashita, A. Hori, and B. Mizuno, Proc. IEDM-1997, p. 475 (1997).

[5] J. R. Conrad, J. L. Radtke, R. A. Dodd, F. J. Worzala, and N. C. Tran, J. Appl. Phys., **62**, 4591 (1987).

[6] P. K. Chu, S. Qin, C. Chan, N. W. Cheung, and L. A. Larson, Mat. Sci. Eng. Reports, **R17(6-7)**, 207 (1996).

[7] Z. Fan, Q. C. Chen, P. K. Chu, and C. Chan, IEEE Trans. Plasma Sci., **26(6)**, 1661 (1998).

[8] Z. Fan, P. K. Chu, N. W. Cheung, and C. Chan, IEEE Trans. Plasma Sci., **27(2)**, 633 (1999).

[9] Z. Fan, X. C. Zeng, D. T. K. Kwok, and P. K. Chu, IEEE Trans. Plasma Sci (February 2000).

[10] D. T. K. Kwok, P. K. Chu, and C. Chan, IEEE Trans. Plasma Sci., **26(6)**, 1669 (1998).

[11] D. T. K. Kwok, P. K. Chu, B. P. Wood, and C. Chan, J. App. Phys., **86(4)**, 1817 (1999).

[12] J. F. Ziegler, J. P. Biersack and U. Littmark, in "*The Stopping and Range of Ions in Solids*", Pergamon Press, New York, 1985.

[13] P. Kellerman, presented at the European Ion Implantation Users Group Meeting, Erlanger, Germany, Nov 18 & 19, 1999.

[14] E. C. Jones, W. En, S. Ogawa, D. B. Fraser, and N. W. Cheung, J. Vac. Sci. Technol. B, **12(2)**, 956 (1994).

[15] P. K. Chu, S. Qin, C. Chan, N. W. Cheung, and L. A. Larson, Mat. Sci. Eng. Reports, **R17(6-7)**, 207 (1996).